JOURNAL OF Materials CHEMISTRY

Self-assembly of alkane capped silver and silica nanoparticles

Håkan Rensmo,[a] Andrea Ongaro,[c] Declan Ryan[b] and Donald Fitzmaurice*[c]

[a]*Department of Physics, University of Uppsala, Box 530, 751 21 Uppsala, Sweden*
[b]*Department of Chemistry and Chemical Biology, Harvard University, 12 Oxford St., Cambridge, MA 02138,, USA*
[c]*Department of Chemistry, National University of Ireland—Dublin, Belfield, Dublin 4, Ireland*

Received 29th April 2002, Accepted 10th June 2002
First published as an Advance Article on the web 30th July 2002

Silver and silica nanoparticles stabilised by long chain alkanes have been prepared and characterised using ^{1}H-NMR, transmission electron microscopy (TEM) and small-angle X-ray scattering (SAXS). Upon solvent evaporation, the alkane stabilised silica and silver nanoparticles self-assemble into close-packed two- and three-dimensional structures. Furthermore, it is shown that a mixture of large silica (90 Å) and small silver (48 Å) nanoparticles self-assemble into mixed well-defined close-packed structures. It has been demonstrated that particle size, core material and solvent composition can be employed to control the forces between individual nanoparticles and, consequently, the structure of the self-assembled arrays. These mixed structures have also been studied using UV-visible spectroscopy and their collective optical properties are shown to depend on their overall composition.

Introduction

Partly motivated by the search for new strategies to achieve further miniaturisation of electronic and magnetic data processing and storage devices, the development of facile means to synthesise and arrange matter on a nanometer length scale is an important goal. One such strategy is to use solution phase nanoparticles and self-assemble them, by solvent evaporation, into mesoscopic architectures. Such a strategy relies on the successful preparation of size monodisperse nanocrystals and on a fundamental understanding of their physical properties.[1–9] It also relies on a fundamental understanding of the interparticle interactions controlling self-assembly upon solvent evaporation and how the resulting nanoparticle structure relates to their collective properties.

While the self-assembly phenomena and collective properties of arrays consisting of one type of nanoparticle have been studied by many groups,[7,8,10–22] there have been few reports describing the self-assembly and collective properties of arrays of more than one type of nanoparticle.[23] Accordingly, we have studied the self-assembly and self-organization of long-chain alkane capped silver and silica nanoparticles. These materials were favoured because of the large difference in polarisability and because it proved possible to prepare capped nanoparticles with well-defined sizes that were soluble in a range of organic solvents. In the course of this study, insights have been gained into the factors (nanoparticle material, nanoparticle size and solvent properties) controlling mixed nanoparticle self-assembly and, in turn, the collective properties of the resulting nanoparticle arrays.

Experimental

Sample preparation

Monodisperse samples of dodecanethiol capped silver nanoparticles were prepared using previously reported methods.[10,20] Dodecanol capped silica particles were prepared by etherification of the surface silanol groups with dodecanol ($C_{12}H_{25}OH$).[24–28] Briefly, an acidified (H_2SO_4, pH = 2) aqueous dispersion (10 mL) of silica nanoparticles (10% by wt, Ludox® SM30) was mixed with ethanol (99.5%, 4 × 50 mL) and the water removed by azeotropic distillation. At this point dodecanol (50 mL) was added to the ethanolic dispersion (50 mL), and the ethanol removed by distillation. The silica nanocrystals were capped with dodecanol by heating the above dispersion to 170 °C for 2 h under nitrogen. The dodecanol capped silica particles formed as a result were precipitated by addition of ethanol, recovered by centrifugation and washed thoroughly with chloroform. The size-polydisperse silica nanoparticles were re-dispersed in chloroform or hexane and size-selectively precipitated by the addition of ethanol.

Organised arrays of the alkane capped silica and silver nanoparticles were formed by evaporating the chloroformic dispersion of nanoparticles (0.5 mg mL^{-1}) on a carbon-coated copper grid or a mica substrate. All ratios for the self-assembled mixed layers are quoted in terms of relative particle number in the dispersion.

Sample characterisation

TEM was performed using a JEOL JEL-2000 EX electron microscope operating at 80 kV. Optical absorption spectra were measured using a Hewlett-Packard 8452A diode array spectrometer. ^{1}H-NMR spectroscopy was performed using a JEOL JNM-GX270 FT spectrometer.

Small-angle X-ray scattering (SAXS) data were obtained on Beam Line 8.2 of the Synchrotron Radiation Source (SRS) at the Daresbury Laboratory, Warrington, UK and on Beam Line ID1 at the European Synchrotron Source (ESRF), Grenoble, France (λ = 1.54 Å). The data was analysed using the expressions below.[10,14,29,30]

The intensity, $I(q,r)$, of scattering at q value, $q = \frac{4\pi}{\lambda}\sin(\theta)\frac{\pi}{2}$, for spherical particles with a radius r can be expressed as a function of scattering intensity, $\Delta\rho_e$, volume of scatter, V_{np}, the shapefactor, $P(q,r)$, and the interparticle scattering factor, $S(q,r)$.

$$I(q,r) = \Delta\rho_e^2 V_{np}^2 P(q,r) S(q,r) \quad (1)$$

For non-interacting spherical particles of uniform density, $S(q) = 1$. The scattering intensity for polydisperse spheres can then be obtained by integrating $I(q,r)$ over the size distribution (a Gaussian distribution of radius r_m and standard deviation σ was used here)

 DOI: 10.1039/b204057c

$$I(q,r) = \Delta\rho_e^2 V_{np}^2 \int_0^\infty \frac{1}{\sigma\sqrt{2\pi}} \exp\left[\frac{-(r-r_m)^2}{2\sigma^2}\right] P(q,r) r^6 dr \quad (2)$$

where,

$$P(q,r) = \left[3\frac{\sin(qr) - qr\cos(qr)}{(qr)^3}\right]^2 \quad (3)$$

For interacting particles $S(q) \neq 1$, and for an array of particles having long-range order, $S(q)$ depends on the superlattice structure. For example, indexing the peaks as a face-centered cubic (FCC) structure, the (111) peak, q_{111}, can be used to measure the *CC* (center-to-center) distance:

$$CC = \frac{2\pi}{q_{111}\cos(30^\circ)} \quad (4)$$

For a less ordered structure $S(q)$ can be used to calculate the radial distribution function, $g(r)$:

$$g(r) - 1 \propto \frac{1}{r}\int q[S(q) - 1]\sin(qr)dq \quad (5)$$

Results and discussion

Nanoparticle characterisation

The dodecanethiol capped silver nanoparticles used in the present study, and shown in Fig. 1a, have been characterised as described in detail elsewhere.[10,14] These nanoparticles are best described as "soft spheres", having an effective diameter equal to the diameter of the nanoparticle core and the densely packed dodecanethiol layers. Unlike hard spheres—particles that exhibit a sharp infinitely strong repulsion upon touching—the soft spheres employed in the present study exhibit a gradually increasing repulsion due to the forces that act between the stabilising ligands and an attraction due to the van der Waals (vdW) forces that act between the solid metallic cores.[10,14]

The findings of a similar study of the dodecanol capped silica nanoparticles are presented below.

Shown in Fig. 1b is the TEM image obtained for dodecanol capped silica nanoparticles. Observed are two-dimensional hexagonally close-packed arrays of nanoparticles in which the constituent nanoparticles are separated from their nearest neighbours by an interspersed dense alkane monolayer. It should be noted that the irregular shape of these nanoparticles prevent long-range ordering. Sizing these particles, assuming they are spherical, gives an average core diameter of 95 $\pm$ 12 Å and an average surface-to-surface interparticle spacing of about 15 Å.

^{1}H-NMR studies of the dodecanol capped silica nanoparticles confirm the presence of alkane chains at the surface, see Fig. 2. The resonances of the chemisorbed dodecanol molecules can be correlated with the resonances observed for the same compound in solution.[31] The observed broadening is most likely a result of the restricted motion of these chains compared to their solution state.

Elemental analysis reveals an organic content of 15% for the dodecanol capped silica nanoparticles. Based on an average nanoparticle core diameter of 90 Å, obtained from SAXS (see below), it is estimated that there are an average of 500 molecules adsorbed at the surface of each nanoparticle and that each molecule occupies an area of 50 Å^2, which is similar to previously published values.[32]

As has been previously reported for the silver nanoparticles, SAXS can be used to obtain a more statistically sound and, in some respects, complementary representation of the average nanoparticle core diameter and the superlattice structure[10,14,29] (see Experimental section).

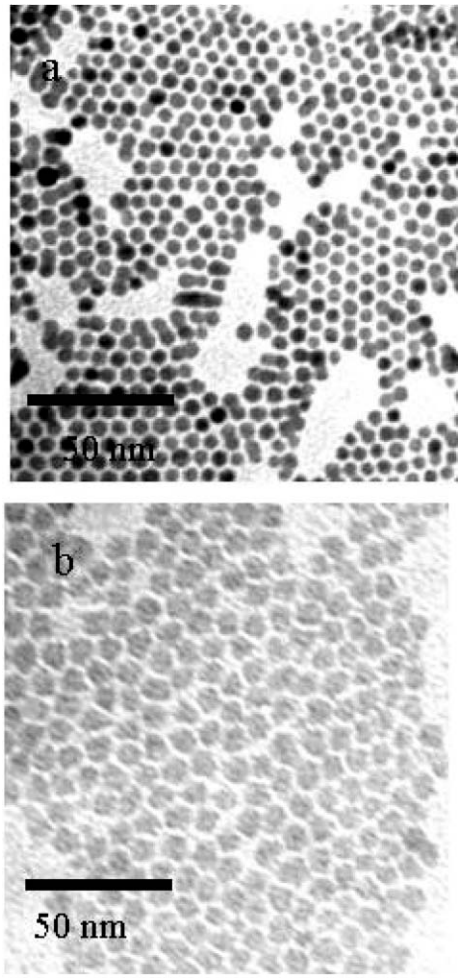

Fig. 1 TEM images of two-dimensional hexagonally close-packed monolayers formed by evaporating chloroformic dispersions of size-monodisperse nanoparticles (about 0.5 mg mL^{-1}) on a carbon coated grid. (a) Dodecanethiol capped silver nanoparticles with an average core diameter of 48 Å and an average centre-to-centre distance of 63 Å. (b) Dodecanol capped silica nanoparticles with an average core diameter of 95 Å and an average centre-to-centre distance of 110 Å.

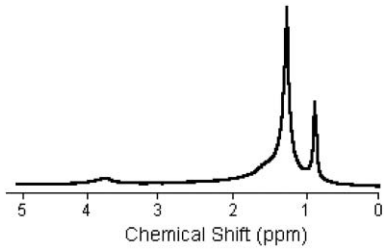

Fig. 2 ^{1}H-NMR of dodecanol capped silica nanoparticles in chloroform-*d*.

Fig. 3 shows a typical scattering profile and the corresponding Porod plot (Iq^4 *vs.* q) for a dispersion in hexane of dodecanol capped silica nanoparticles. At lower scattering angles the scattering oscillates with q while the presence of a distribution of particle sizes damps the oscillation at higher scattering angles. Using eqn. (2) it is possible to fit the curve for an average nanoparticle diameter of 90 $\pm$ 14 Å. This value reflects the diameter of the silica nanoparticle core alone since the electron density is very similar for the alkane chains and hexane. This value agrees well with the value of 95 Å obtained from an analysis of the TEM image in Fig. 1b.

The SAXS profile of three-dimensional films of dodecanol capped silica nanoparticles prepared by hexane evaporation

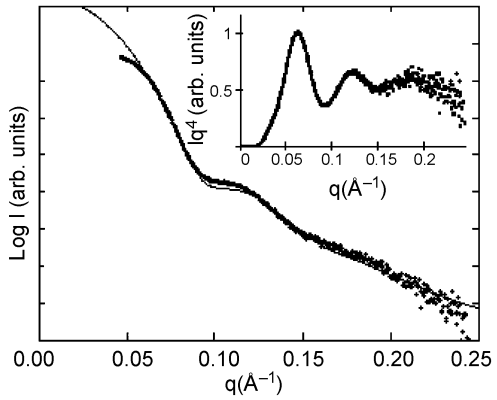

Fig. 3 SAXS spectra of dodecanol capped silica nanoparticles in hexane (1 mg mL^{-1}). The curve represents the best fit of the data as discussed in the text. The inset shows a Porod plot of the same data.

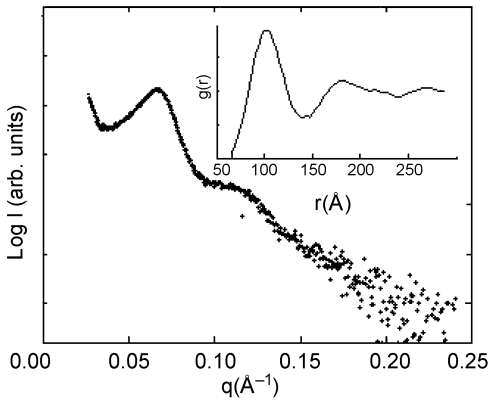

Fig. 4 SAXS spectra of dodecanol capped silica nanoparticles self-assembled on a mica substrate. The inset shows the radial distribution function, $g(r)$, obtained from the same data.

displays two major peaks indicative of medium-range order as expected from the TEM image above, see Fig. 4. The data in Fig. 4 was analysed assuming an amorphous structure having a characteristic radial distribution function $g(r)$, see eqn. (5). The function $g(r)$ indicates the probability of finding a particle at a distance r from another central particle. On this basis a value for the interparticle spacing of 103 Å is obtained, see inset to Fig. 4. Together with the SAXS data obtained above, from which a value of 90 Å for the average core diameter was obtained, this result suggests an interparticle spacing of 13 Å. This value for the interparticle spacing also agrees well with the value of 15 Å obtained from an analysis of the TEM images in Fig. 1b.

While the self-assembly of silver nanoparticles has been shown to be affected by the long-range attractive vdW forces that act between the silver core,[10,14,33] the influence of these attractive forces (other attractive forces due to specific interactions between the capping molecules may still be present) are less pronounced during self-assembly of alkane capped silica nanoparticles.[26] Despite this, dodecanol capped silica nanoparticles self-assemble to form structures very similar to those formed by the dodecanethiol capped silver nanocrystals upon solvent evaporation. That is, the silica and silver nanoparticles studied here consist of a solid core capped by an alkane layer which, during solvent evaporation, maintains the separation between the nanoparticle cores. In both cases the steric stabilisation and associated repulsive forces are sufficient to provide the entropic freedom necessary for ordering to occur.

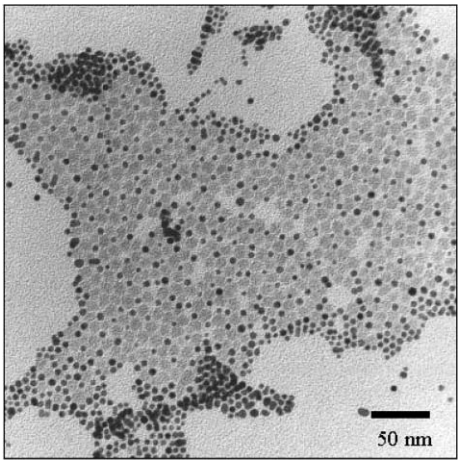

Fig. 5 A TEM image of two-dimensional self-assembled mixed monolayers formed by evaporating a 2 : 1 mixed chloroformic dispersion of dodecanethiol capped silver nanoparticles (48 Å core diameter, centre-to-centre distance of 63 Å) and dodecanol capped silica nanoparticles (95 Å, centre-to-centre distance of 110 Å).

Self-assembling mixed arrays

The binary arrays studied were prepared by evaporating mixed dispersions of silver and silica nanoparticles on suitable substrates. Initially small silver nanoparticles (average core diameter of 48 $\pm$ 5 Å, see Fig. 1a) were used in order to minimise the attractive vdW forces between the metal cores.

A drop of a binary dispersion (2 : 1) of silver (average core diameter of 48 Å) and silica (average core diameter of 90 Å) nanoparticles was placed on the surface of a carbon coated copper grid and the solvent allowed to evaporate, see Fig. 5. From the resulting TEM image it is clear that the silver and silica nanoparticles self-assemble to form a mixed two-dimensional well defined close-packed array. Despite the fact that the array is not perfectly ordered, this finding strongly supports the view that, because the effects of the attractive forces acting between the silver nanoparticles have been minimised, the steric stabilisation and associated repulsive forces of both the silver and silica nanoparticles are sufficient to provide the entropic freedom necessary for ordering. The mixed nanoparticle array is surrounded by a halo of silver nanopaticles, presumably a consequence of there being an excess of silver nanoparticles.

SAXS was also used to investigate the above binary nanoparticle array. The scattering profile for such an array will depend not only on interparticle correlations from one type of particle but also on the contributions from interparticle correlations between two types of nanoparticles. It is expected that this will be the case because scattering from a particle is dependent on its electron content ($\Delta\rho_e V_{np}$), which for the silver and silica nanoparticles used above is very similar. The SAXS profile of the binary nanoparticle array, formed by placing a drop of the binary nanoparticle dispersion on a mica substrate and allowing the solvent evaporate, is shown in Fig. 6 together with the profile of self-assembled arrays formed from dispersions containing the silver and silica particles alone. The profile measured for the silver nanoparticle arrays reveals a scattering peak at 0.120 Å^{-1}, while the larger silica nanoparticles give rise to a peak at 0.066 Å^{-1}. These values correspond, assuming an FCC lattice structure, to a center-to-center distance of 61 Å for silver nanoparticles and 110 Å for the silica nanoparticles. As might have been expected, the profile of the 2 : 1 mixture shown in Fig. 6 is different from that measured for both the silver and the silica nanoparticles and is different from a superposition of the two. In the profile obtained for the 2 : 1 mixture new scattering peaks are measured at 0.040 Å^{-1} and 0.083 Å^{-1}, corresponding to center-to-center distances of 180 Å

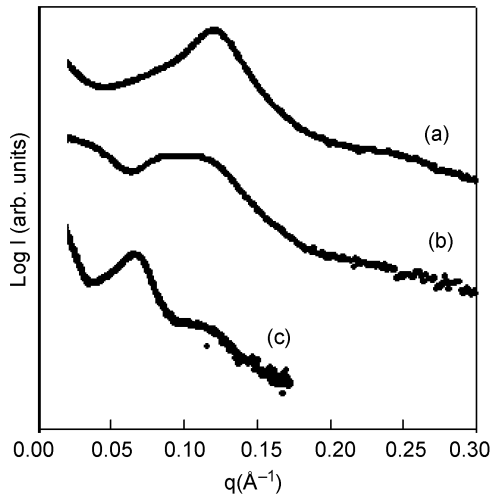

Fig. 6 SAXS spectra of self-assembled arrays of (a) 48 Å silver nanoparticles, (b) a 2 : 1 mixture of 48 Å silver and 90 Å silica nanoparticles (c) 90 Å silica nanoparticles.

and 87 Å respectively [eqn. (4)]. The value of 180 Å is in reasonable agreement with the center-to-center distance of 171 Å expected for two silver nanoparticles separated by the diameter of a silica nanoparticle, while 87 Å approximates the center-to-center distance expected between a silver and silica nanoparticle. Although the usefulness of a simple quantitative analysis like this is predicated on the assumption of a perfect FCC superlattice, the SAXS spectrum of the three-dimensional arrays in Fig. 6 is nevertheless consistent with the TEM image presented in Fig. 5.

A more sophisticated analysis can be performed on a scattering profile measured for a binary array in which scattering from one type of nanoparticle completely dominates. This dominance can be achieved by increasing the diameter and number of the silver nanoparticles. Experimental form factors (obtained from silver nanoparticles dispersed in solution) can then be used to calculate the static structure factor, $S(q)$, and subsequently the radial distribution function, $g(r)$, using eqn. (5). The SAXS scattering profile obtained for nanoparticle arrays prepared by evaporating dispersions of silver (average core diameter of 64 Å), silica (average core diameter of 90 Å) and binary mixtures (40 : 1) of silver and silica nanoparticles is shown in Fig. 7a. As expected, the very monodisperse silver nanoparticles order to give an FCC superlattice. The presence of a relatively small number of silica nanoparticles within this superlattice is reflected in the broadening of the silver (111) peak. The radial distribution function, $g(r)$, was calculated from the profile in Fig. 7a in an attempt to quantify the extent of mixing, see Fig. 7b. The $g(r)$ calculated for the array formed by evaporation of the mixed dispersion correlates at shorter distances with the spectra calculated from the array formed by evaporation of the silver nanoparticle dispersion, while differences are clearly seen at longer distances. For a perfectly close packed FCC superlattice, the first coordination shell contains six particles, the second twelve and the third twenty-four. Therefore, if the silica nanoparticles randomly mix into the silver superlattice, effects assigned to lattice defects (induced by a 40 : 1 ratio of silver to silica nanoparticles) should be seen from the third coordination shell and beyond. The spectra in Fig. 7b are, therefore, entirely consistent with this view and indicate a statistical mixing of the silica nanoparticles within the silver superlattice.

In summary, the above analyses of binary arrays formed by evaporation of dispersions of silver (either 48 Å or 64 Å average core diameter) and silica (90 Å average core diameter) nanoparticles support the following view: in the cases where the attractive forces acting between nanoparticles are relatively

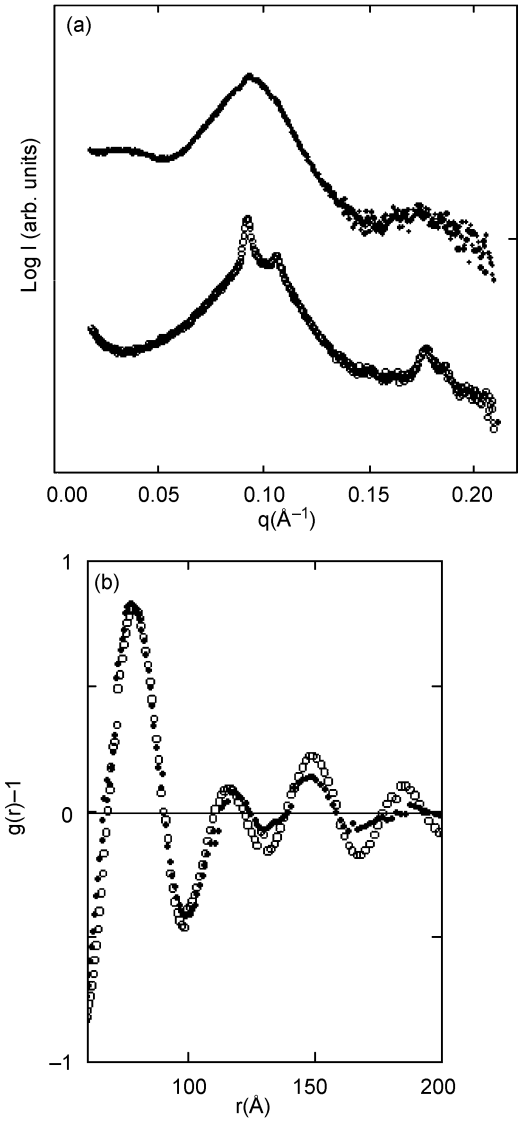

Fig. 7 (a) SAXS spectra of self-assembled arrays of 64 Å silver nanoparticles (circle) and a 40 : 1 mixture of 64 Å silver and 90 Å silica nanoparticles (dot). (b) Radial distribution functions calculated from the SAXS spectra in (a) of self-assembled arrays of 64 Å silver nanoparticles (circle) and a 40 : 1 mixture of 64 Å silver and 90 Å silica nanoparticles (dot).

small, and the repulsive forces acting between particles are sufficient to provide the entropic freedom for ordering, then the self-assembly of unmixed compared to mixed nanoparticle arrays will be largely indistinguishable.

Optical properties of mixed arrays

In the context of the above discussion, it is noted that silver nanoparticles show an intense optical absorption that is assigned to the collective oscillations of free electrons, *i.e.* surface plasmon resonance. The wavelength at which the resonance is observed depends not only on the size and shape of the individual particles, but also on the relative permittivity of the surrounding media.[18,34–37]

Shown in Fig. 8 is the optical absorption spectrum of a dispersion of dodecanethiol capped silver nanoparticles (average core diameter of 48 Å) in chloroform, together with the spectrum of the three-dimensional nanoparticle array formed by evaporation of the same dispersion. The measured spectra are dominated by a visible absorption band assigned to a surface plasmon resonance. The red-shifted band observed for the three-dimensional silver nanoparticle array is accounted

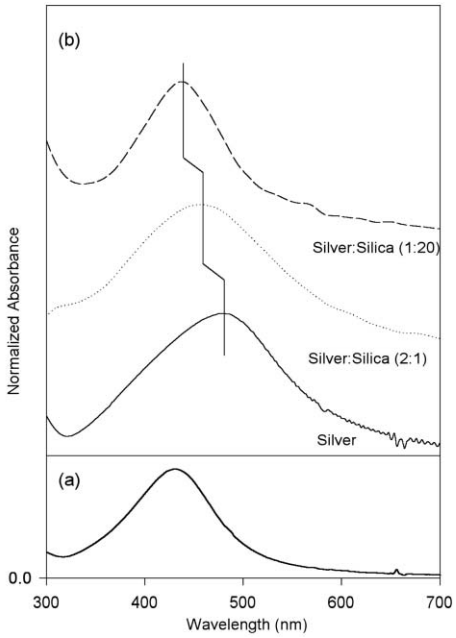

Fig. 8 (a) Optical absorption spectra of a chloroformic dispersion of size-monodisperse dodecanethiol capped silver nanoparticles (48 Å, about 0.03 mg mL^{-1}). (b) Optical absorption spectra of three-dimensional close-packed arrays formed by evaporating chloroformic mixed dispersions of dodecanethiol capped silver nanoparticles (48 Å core diameter) and dodecanol capped silica nanoparticles (90 Å core diameter) on mica (about 0.5 mg mL^{-1}). The relative proportions of silver and silica nanoparticles were as indicated.

for by an increase in the effective relative permittivity of the surrounding medium.[18,34–37]

Also shown in Fig. 8 are the optical absorption spectra of three-dimensional binary nanoparticle arrays formed by evaporation of the following binary nanoparticle dispersions: a 2 : 1 mixture of silver (average core diameter of 48 Å) and silica (average core diameter of 90 Å) nanoparticles and a 1 : 20 mixture of the same silver and silica nanoparticles. The TEM image and SAXS profile (Figs. 5–7) of the two-dimensional binary array (2 : 1) suggests that the silver nanoparticles are largely "dispersed" among the silica nanoparticles and, as a consequence, that the plasmon band ought to be observed at a wavelength between that of the silver nanoparticle dispersion and the three-dimensional silver nanoparticle array. As the plasmon resonance is observed at 456 nm this expectation is clearly well founded. Furthermore, dilution of the silver nanoparticles in the three-dimensional binary array formed by evaporation of the 1 : 20 mixed nanoparticle dispersion yields a plasmon band at 437 nm, *i.e.* very close to that of the silver nanoparticle dispersion. In short, the electronic properties of a self-assembled layer formed by solvent evaporation of the silver and silica nanoparticles can be readily tuned in a controlled manner.

Controlling the assembly of mixed binary arrays

While statistical mixing of the two nanoparticles allows for tuning of the optical spectra of a binary nanoparticle array by varying the relative nanoparticle concentrations, other means by which the structure of a binary nanoparticle array and accordingly its collective optical properties can be controlled are of importance for more advanced applications. To successfully develop such means, an understanding of the factors that determine the magnitude of the attractive and repulsive forces during self-assembly of a nanoparticle array are important.

The long-range attractive vdW forces acting between nanoparticles depend on the average core diameter of the nanoparticle and on differences in the polarisabilities of nanoparticle core material and on the solvent in which the nanoparticles are dispersed. The short-range repulsive forces acting between two nanoparticles depend on the extent of coverage on the nanoparticle core by the stabiliser and on the properties (length, flexibility, *etc.* of the stabiliser). It should be noted that the factors which affect the long- and short-range forces that act between nanoparticles also affect the forces that act between a nanoparticle and the solvent medium and, upon solvent evaporation, between a nanoparticle and the substrate on which the nanoparticles are deposited.[24–27] Accordingly, if the composition or the dimensions of the nanoparticle core, the nature of the stabiliser or the extent of its coverage, or the solvent medium are altered this will affect the nature of the binary nanoparticle array that is self-assembled upon solvent evaporation.

In the remaining paragraphs of this section we present the findings of a study which has provided insights into how changing the dimensions of one of the cores or one of the nanocrystals in a binary nanocrystal mixture affects the structure of the nanoparticle array which is self-assembled. Also presented are the findings of a related study that has provided insights into how changing the solvent medium affects the structure and, consequently, the properties of the nanoparticle array that is self-assembled.

It has previously been shown that size-polydisperse gold nanoparticles, stabilised by an adsorbed monolayer of dodecanethiol molecules, form opals.[33] This finding was accounted for by the size-dependence of attractive vdW forces acting between the gold nanoparticles.

As discussed above and when reporting the finding of a study of the binary nanoparticle arrays formed by a 2 : 1 mixture of silver (average core diameter of 48 Å) and silica (average core diameter of 90 Å) dispersed in chloroform, the silver nanocrystals are sufficiently small to ensure that the attractive vdW forces acting between the nanoparticles are minimised and that there is enough entropic freedom to allow the silver and silica nanoparticles to form the expected array, see Fig. 5. The above experiment was repeated for a 1 : 1 mixture of silver (average core diameter of 80 Å) and silica (average core diameter of 90 Å) nanoparticles, see Fig. 9. In this case the silver nanoparticles are not sufficiently small to ensure that the attractive vdW forces acting between the nanoparticles are minimised so that there is enough entropic freedom to allow the silver and silica nanoparticles to form the expected array in which the array sites are randomly occupied by either a silver or silica

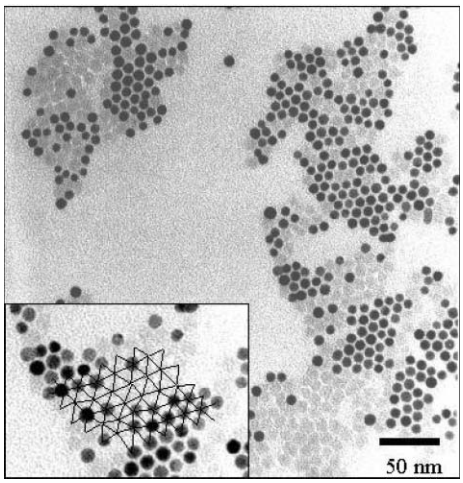

Fig. 9 A TEM image of two-dimensional self-assembled mixed monolayers formed by evaporating a 1 : 1 mixed chloroformic dispersion of dodecanethiol capped silver nanoparticles (80 Å core diameter, centre-to-centre distance of 95 Å) and dodecanol capped silica nanoparticles (95 Å, centre-to-centre distance of 110 Å) determined by TEM.

nanoparticle. Instead, as is clearly the case from the TEM shown in Fig. 9, the silver and, therefore also the silica, nanoparticles self-associate and self-assemble into a close-packed binary nanoparticle array comprised of domains of close-packed silver and domains of close-packed silica nanoparticles.

The role of the solvent in determining the nature of the binary nanoparticle array formed upon solvent evaporation is considered next. Adding small amounts of ethanol (a non-solvent) to a chloroformic dispersion of dodecanethiol capped silver nanoparticles prior to solvent evaporation leads to self-assembly of a three-dimensional, rather than a two-dimensional, nanoparticle array. As seen in Fig. 10, bilayers are formed after addition of about 5% (by volume) of ethanol and multilayers are formed after addition of 10% (by volume) of ethanol. These results, as expected, are in quantitative agreement with those reported earlier for gold nanocrystals.[11] A similar study reveals qualitatively similar behaviour for silica nanoparticles, see Fig. 10. However, the change from two-dimensional to three-dimensional arrays occurs in the case of silica nanoparticles after adding larger percentages of ethanol to the solution. Bilayers are only seen after about 30% addition while multilayer formation is seen after 40% addition.

The quantitative difference in multilayer formation upon non-solvent addition between the two types of nanoparticles may now be used to control the architecture of the binary nanoparticle array. This approach is demonstrated, in Fig. 11, by showing the binary arrays formed upon solvent evaporation after addition of 5% and 10% ethanol to a binary nanoparticle dispersion. As expected, 10% addition yields multilayers of the silver nanoparticles while the silica nanoparticles still form monolayers. The result demonstrates one way in which the structure of a self-assembled three-dimensional binary array formed upon solvent evaporation can be controlled.

Also of interest, however, is the fact that smaller amounts of ethanol (too small to yield three-dimensional growth) also affects the two-dimensional binary arrays. For example, after 5% addition of ethanol it is seen that the nanoparticles separate from each other to form large domains consisting of only one type of nanoparticle, see Fig. 11. That is, the balance between the forces acting between the different nanoparticles, between the nanoparticles and the solvent and between the nanoparticles and the substrate can be easily altered to control the self-assembled structure.

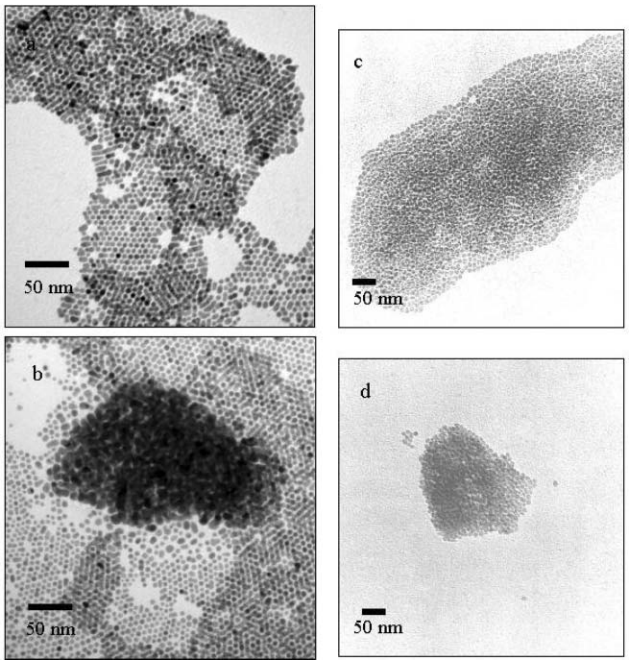

Fig. 10 A TEM image of two- and three-dimensional self-assembled monolayers formed by evaporating chloroformic/ethanolic dispersions of silver or silica nanoparticles onto a carbon coated copper grid. (a) 64 Å silver nanoparticles evaporated from a chloroform/ethanol mixture (5% ethanol), (b) 64 Å silver nanoparticles evaporated from a chloroform/ethanol mixture (10% ethanol), (c) 90 Å silica nanoparticles evaporated from a chloroform/ethanol mixture (5% ethanol) and (d) 90 Å silica nanoparticles evaporated from a chloroform/ethanol mixture (10% ethanol).

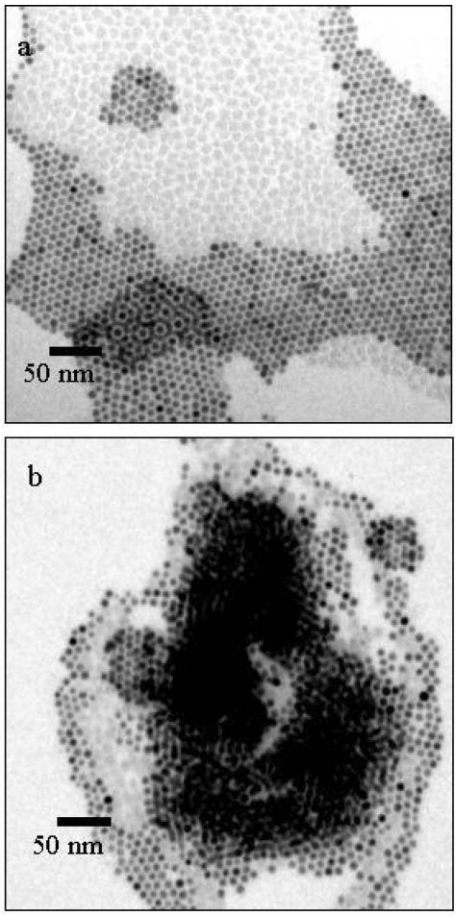

Fig. 11 A TEM image of two- and three-dimensional self-assembled mixed monolayers formed by evaporating a 1 : 1 mixed dispersion of dodecanethiol capped silver nanoparticles (64 Å core diameter) and dodecanol capped silica nanoparticles (90 Å core diameter). (a) Evaporated from a chloroform/ethanol mixture (5% ethanol). (b) Evaporated from a chloroform/ethanol mixture (10% ethanol).

Finally, the collective properties of these arrays were studied by UV-visible spectroscopy. As discussed above, it was expected that the change in structure due to addition of ethanol would correspond to a change in the absorption spectra of the three-dimensional binary array. As seen in Fig. 12 this expectation is well founded. The absorption spectrum, of the binary array formed by evaporation of a chloroformic dispersion (1 : 1 ratio of 64 Å silver and 90 Å silica nanoparticles) onto the mica substrate, shows a peak at 456 nm while after adding 5% ethanol to the dispersion the spectrum is broadened with a contribution at longer wavelengths from what is most likely close-packed regions of silver nanocrystals. These spectra therefore support the TEM results (Fig. 11) and again also demonstrate control over the three-dimensional structure formed during solvent evaporation of a mixed dispersion as well as control over its collective properties.

Conclusions

Nanoparticles that are stabilised with long chain alkanes self-assemble into ordered arrays upon solvent evaporation.

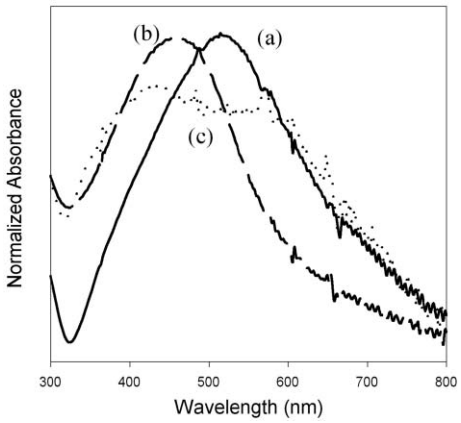

Fig. 12 Optical absorption spectra of three-dimensional close-packed arrays formed by evaporating chloroformic dispersion on mica of (a) dodecanethiol capped silver nanoparticles (b) a 2 : 1 mixed dispersion of dodecanethiol capped silver nanoparticles (64 Å core diameter) and dodecanol capped silica nanoparticles (90 Å core diameter). Also shown (c) is the optical absorption spectra of three-dimensional close-packed arrays formed by evaporating a chloroformic/ethanolic (5% ethanol) dispersion of the same solution as in (b) on mica.

Here, it is shown that large silica nanoparticles (average core diameter of 90 Å) and small silver nanoparticles (average core diameter of 48 Å) self-assemble into well-defined binary close-packed arrays. This is expected as, upon solvent evaporation, the gradually increasing repulsion, induced by the adsorbed alkane chains, limits the attraction between all constituent nanoparticles allowing a sufficient number of configurations to be sampled to ensure that entropically favoured binary arrays are formed.

It has also been observed that mixing silica nanoparticles (90 Å core diameter) with larger silver nanoparticles (80 Å core diameter), results in self-assembly of the silica or silver nanoparticles into domains consisting of only one type of nanoparticle. This observation suggests that during solvent evaporation the long-range vdW forces enhances the attraction between the silver nanoparticles. These nanoparticles still, however, remain capable of sampling a sufficient number of configurations so that the favoured minimum free energy structure is formed. This result demonstrates how the structures of mixed self-assembled nanoparticle arrays are affected by changing the size of the nanoparticles.

It has further been demonstrated how the structures of the binary arrays can be altered by the addition of a non-solvent, in this case ethanol, to a chloroformic dispersion of silver and silica nanoparticles. Specifically, upon addition of ethanol, the mixed nanoparticle array separates into domains consisting of only one type of nanoparticle. These structural changes have been shown to result in changes in the collective properties of these binary arrays.

In conclusion, these results are of specific interest since they demonstrate that the composition and dimension of the nanoparticle core and the solvent composition are key factors that affect the binary nanoparticle arrays and, in turn, their collective optical properties.

These findings are of general interest as they point toward the self-assembly, in solution or at technologically relevant substrates, of complex nanostructured materials with well-defined structures and properties.

Acknowledgements

The authors acknowledge the support of the American Chemical Society (Petroleum Research Fund) and helpful discussions with D. Cottell. HR acknowledges support from STINT (The Swedish Foundation for International Co-operation in Research and Higher Education).

References

1 D. V. Leff, P. C. Ohara, J. R. Heath and W. M. Gelbart, *J. Phys. Chem.*, 1995, **99**, 7036–7041.
2 A. P. Alivisatos, *Science*, 1996, **271**, 933–937.
3 T. Vossmeyer, L. Katsikas, M. Giersig, I. G. Popovic, K. Diesner, A. Chemseddine, A. Eychmueller and H. Weller, *J. Phys. Chem.*, 1994, **98**, 7665–7673.
4 N. Herron, J. C. Calabrese, W. E. Farneth and Y. Wang, *Science*, 1993, **259**, 1426–1428.
5 G. Schmid, *Chem. Rev.*, 1992, **92**, 1709–1727.
6 T. Moritz, J. Reiss, K. Diesner, D. Su and A. Chemseddine, *J. Phys. Chem. B*, 1997, **101**, 8052–8053.
7 C. P. Collier, T. Vossmeyer and J. R. Heath, *Annu. Rev. Phys. Chem.*, 1998, **49**, 371–404.
8 C. B. Murray, C. R. Kagan and M. G. Bawendi, *Science*, 1995, **270**, 1335–1338.
9 R. L. Whetten, J. L. Khoury, M. M. Alvarez, S. Murthy, I. Vezmar, Z. L. Wang, P. W. Stephens, C. L. Cleveland, W. D. Luedtke and U. Landman, *Adv. Mater.*, 1996, **8**, 428.
10 B. A. Korgel and D. Fitzmaurice, *Phys. Rev. B*, 1999, **59**, 14191–14201.
11 B. A. Korgel and D. Fitzmaurice, *Phys. Rev. B: Condens. Matter*, 1998, **80**, 3531–3534.
12 L. Motte, F. Billoudet, E. Lacaze, J. Douin and M. P. Pileni, *J. Phys. Chem. B*, 1997, **101**, 138–144.
13 L. Motte and M. P. Pileni, *J. Phys. Chem. B*, 1998, **102**, 4104–4109.
14 B. A. Korgel, S. Fullam, S. Connolly and D. Fitzmaurice, *J. Phys. Chem. B*, 1998, **102**, 8379–8388.
15 S. A. Harfenist, Z. L. Wang, M. M. Alvarez, I. Vezmar and R. L. Whetten, *J. Phys. Chem.*, 1996, **100**, 13904–13910.
16 S. Connolly, S. Fullam, B. Korgel and D. Fitzmaurice, *J. Am. Chem. Soc.*., 1998, **120**, 2969–2970.
17 B. A. Korgel, N. Zaccheroni and D. Fitzmaurice, *J. Am. Chem. Soc.*, 1999, **121**, 3533–3534.
18 J. R. Heath, C. M. Knobler and D. V. Leff, *J. Phys. Chem. B*, 1997, **101**, 189–197.
19 C. B. Murray, D. J. Norris and M. G. Bawendi, *J. Am. Chem. Soc.*, 1993, **115**, 8706–8715.
20 M. Brust, M. Walker, D. Bethell, D. J. Schiffrin and R. Whyman, *J. Chem. Soc., Chem. Commun.*, **1994**, 801–802.
21 M. J. Hostetler, J. E. Wingate, C. J. Zhong, J. E. Harris, R. W. Vachet, M. R. Clark, J. D. Londono, S. J. Green, J. J. Stokes, G. D. Wignall, G. L. Glish, M. D. Porter, N. D. Evans and R. W. Murray, *Langmuir*, 1998, **14**, 17–30.
22 R. P. Andres, J. D. Bielefeld, J. I. Henderson, D. B. Janes, V. R. Kolagunta, C. P. Kubiak, W. J. Mahoney and R. G. Osifchin, *Science*, 1996, **273**, 1690–1693.
23 C. Kiely, J. Fink, M. Brust, D. Bethell and D. J. Schiffrin, *Nature*, 1999, **396**, 444–446.
24 J. W. Jansen, C. G. De Kruif and A. Vrij, *J. Colloid Interface Sci.*, 1986, **114**, 501–504.
25 J. W. Jansen, C. G. De Kruif and A. Vrij, *J. Colloid Interface Sci.*, 1986, **114**, 492–500.
26 J. W. Jansen, C. G. De Kruif and A. Vrij, *J. Colloid Interface Sci.*, 1986, **114**, 471–480.
27 J. W. Jansen, C. G. De Kruif and A. Vrij, *J. Colloid Interface Sci.*, 1986, **114**, 481–491.
28 R. K. Iler, *The Chemistry of Silica*, John Wiley & Sons, New York, 1979.
29 H. Mattoussi, A. W. Cumming, C. B. Murray, M. G. Bawendi and R. Ober, *J. Chem. Phys.*, 1996, **105**, 9890–9896.
30 O. Glatter and O. Kratky, *Small-Angle X-ray Scattering*; Academic Press, New York, 1992.
31 ^{1}H NMR ($CDCl_3$): 0.88 (t, 3H, J = 7.0 Hz), 1.22 (m, 16H), 1.36 (m, 2H), 1.61 (m, 2H), 2.52 (q, 2H, J = 7.0 Hz, J = 3.5 Hz).
32 C. C. Ballard, E. C. Broge, R. K. Iler, D. S. St.John and J. R. McWhorter, *J. Colloid Interface Sci.*, 1999, **65**, 20–25.
33 P. C. Ohara, D. V. Leff, J. R. Heath and W. M. Gelbart, *Phys. Rev. Lett.*, 1995, **75**, 3466–3469.
34 H. Hoevel, S. Fritz, A. Hilger, U. Kreibig and M. Vollmer, *Phys. Rev. B: Condens. Matter*, 1993, **48**, 18178–18188.
35 J. Schmitt, P. Maechtle, D. Eck, H. Moehwald and C. A. Helm, *Langmuir*, 1999, **15**, 3256–3266.
36 S. Underwood and P. Mulvaney, *Langmuir*, 1994, **10**, 3427–3430.
37 M. Brust, D. Bethell, C. J. Kiely and D. J. Schiffrin, *Langmuir*, 1998, **14**, 5425–5429.